

Modular A_4 symmetry and light dark matter with gauged $U(1)_{B-L}$

Keiko I. Nagao^{1,*} and Hiroshi Okada^{2,3,†}

¹*Okayama University of Science, Faculty of Science,*

Department of Applied Physics, Ridaicho 1-1, Okayama, 700-0005, Japan

²*Asia Pacific Center for Theoretical Physics (APCTP) - Headquarters San 31,
Hyoja-dong, Nam-gu, Pohang 790-784, Korea*

³*Department of Physics, Pohang University of Science
and Technology, Pohang 37673, Republic of Korea*

(Dated: August 24, 2021)

Abstract

We propose a radiative seesaw model with a light dark matter candidate (DM) under modular A_4 and gauged $U(1)_{B-L}$ symmetries, in which neutrino masses are generated via one-loop level, and we have a bosonic DM candidate $\sim 0.01 - 50$ GeV. DM is stabilized by nonzero modular weight and a remnant Z_2 symmetry of $U(1)_{B-L}$ symmetry. The naturalness of tiny DM mass is indirectly realized by the radiatively induced mass of neutral fermions that interact with our DM candidate. Thus, DM mass does not have to exceed the neutral fermion masses, whose scale is assumed to be 50 GeV. Taking several benchmark points of DM mass in DM analysis, we show the numerical analysis for the neutrino oscillation data in the normal and inverted hierarchy cases and find several features for both cases.

*Electronic address: nagao@dap.ous.ac.jp

†Electronic address: hiroshi.okada@apctp.org

I. INTRODUCTION

A radiative seesaw model is one of the sophisticated ideas to connect massive neutrinos and dark matter candidate [1], both of which are considered beyond the standard model (SM). Moreover, this model can typically be within a low energy scale \sim TeV, since relatively large Yukawa couplings are expected. Neutrino masses are generated only via interactions of DM at loop levels. This is why we can naturally explain that the neutrino mass is tiny enough without the requirement of small Yukawa couplings. In order to realize this kind of model, we often introduce symmetry in order to stabilize DM in addition to gauge symmetries in SM, and Abelian discrete symmetries (such as Z_2) are frequently applied to this kind of model. Also, flavor physics raises our serious target from this model due to not so small Yukawa couplings. Thus, it would be a natural consequence that stabilized symmetry of DM is extended to a flavor symmetry in order to explain DM and flavor physics at the same time.

Recently, attractive flavor symmetries are proposed by papers [2, 3], in which they applied modular non-Abelian discrete flavor symmetries to quark and lepton sectors. One remarkable advantage is that any dimensionless couplings can also be transformed as non-trivial representations under those symmetries. Therefore, we do not need so many scalars to find a predictive mass matrix. Another advantage is that we have a modular weight from the modular origin that can play a role in stabilizing DM when appropriate charge assignments are distributed to each of the fields of models. Along the line of this idea, a vast reference has recently appeared in the literature, *e.g.*, A_4 [2, 4–38], S_3 [39–44], S_4 [45–56], A_5 [50, 57, 58], double covering of A_5 [59–62], larger groups [63], multiple modular symmetries [64], and double covering of A_4 [65–67], S_4 [68, 69], and the other types of groups [70–75] in which masses, mixing, and CP phases for the quark and/or lepton have been predicted¹. Moreover, a systematic approach to understanding the origin of CP transformations has been discussed in Ref. [84], and CP/flavor violation in models with modular symmetry was discussed in Refs. [85, 86], and a possible correction from Kähler potential was discussed in Ref. [88]. Furthermore, systematic analysis of the fixed points (stabilizers) has been discussed in Ref. [89].

¹ For interest readers, we provide some literature reviews, which are useful to understand the non-Abelian group and its applications to flavor structure [76–83].

	L_{L_i}	e_{R_i}	N_{R_a}	S_{L_a}	S_{R_a}	H	η	φ	χ
$SU(2)_L$	2	1	1	1	1	2	2	1	1
$U(1)_Y$	$-\frac{1}{2}$	-1	0	0	0	$\frac{1}{2}$	$\frac{1}{2}$	0	0
$U(1)_{B-L}$	-1	-1	-1	$-1/2$	$-1/2$	0	0	1	$-1/2$
A_4	{1}	{1}	3	3	3	1	1	1	1
$-k$	0	0	-1^*	-1	0	0	-3	0	-2

TABLE I: Charge assignments of our fields under $SU(2)_L \otimes U(1)_Y \otimes U(1)_{B-L} \otimes A_4 \otimes (-k)$, where $\{\mathbf{1}\} \equiv (\mathbf{1}, \mathbf{1}', \mathbf{1}'')$, $SU(3)_C$ is the same as the SM and singlet for all the new fields, and -1^* indicates complex conjugate of τ should be applied under the modular transformation. $B - L$ charge assignment for the quark sector is $-1/3$ to cancel the chiral anomaly. The lower indices (i, a) are the number of families that runs over 1 – 3.

In this paper, we propose a radiative seesaw model with a modular A_4 and gauged $U(1)_{B-L}$ symmetries, in which the neutrino masses are generated via one-loop level, and we have a relatively light bosonic DM candidate $\sim 0.01 - 50$ GeV. DM is stabilized by nonzero modular weight and a remnant Z_2 symmetry of $U(1)_{B-L}$ symmetry. The naturalness of tiny mass of DM is indirectly realized by the radiatively induced mass of neutral fermions that interact with our DM candidate. Thus, DM mass must not exceed the mass of the neutral fermion masses, whose scale is supposed to be 50 GeV. We numerically analyze our DM candidate and then search for the allowed region of neutrino oscillation data.

This letter is organized as follows. In Sec. II, we review our model, formulating our renormalizable Lagrangian, Higgs potential, and discuss DM including a numerical search for the allowed mass region. Then, we formulate the neutrino sector and show our numerical analysis to satisfy the neutrino oscillation data in cases of normal and inverted hierarchies. In Sec. III, we devote the summary to our results and the conclusion. In the appendix, we briefly review the modular symmetry.

II. MODEL SETUP

In this section, we explain our model.

A. Renormalizable Yukawa Lagrangian and Higgs potential

As for the fermion sector, we introduce three families of right-handed neutral fermions N_R to cancel anomaly coming from gauged $U(1)_{B-L}$ symmetry, where we impose N_R into $(3, -1^*)$ under $(A_4, -k)$. Here, -1^* denotes complex conjugate of τ should be applied under the modular transformation. In addition, we introduce three families of vector-like neutral fermions S_L and S_R with $(-1/2, 3)$ under $(U(1)_{B-L}, A_4)$ that implies $U(1)_{B-L}$ anomaly is automatically cancelled among them. $S_{L,R}$ plays a role in generating the mass of N_R at one loop level. While we impose $(-1, 0)$ charge for (S_L, S_R) under modular weight $-k$. In the quark sector of the SM fermions, we impose $(Q_L, \bar{d}_R, \bar{u}_R) = (3, \{1\}, \{1\})$ under A_4 symmetry and $(-2, 0, -4)$ under the modular weight of $-k$, where $-1/3$ charge is imposed in order to cancel the anomaly of gauged $U(1)_{B-L}$ and $\{\mathbf{1}\} \equiv (\mathbf{1}, \mathbf{1}', \mathbf{1}'')$. Even though we will not discuss masses and mixings on quark sector, there exists allowed region nearby $\tau = i$ or $\tau = i \times \infty$ in ref. [8]. These fixed points are known that there are residual symmetries $Z_2 : \{1, S\}$ and $Z_3 : \{1, T, T^2\}$, respectively.² In the lepton sector of the SM, both L_L and e_R have three types of singlets $\{1\}$ under A_4 with zero modular weight charges. Thanks to their assignments of A_4 symmetry, we find diagonal charged-lepton masses. Therefore, we do not need to diagonalize the mass matrix of charged-leptons at leading order. -1 charge for L_L and e_R is imposed in order to cancel the anomaly of the $U(1)_{B-L}$ that is the same as the typical gauged $U(1)_{B-L}$ symmetry.

As for boson sector, we add an isospin doublet inert boson $\eta \equiv [\eta^+, (\eta_R + i\eta_I)/\sqrt{2}]^T$, two isospin singlets $\varphi \equiv (v' + z' + ir)/\sqrt{2}$ and $\chi \equiv (\chi_R + i\chi_I)/\sqrt{2}$ with $(0, 1, -3)$, $(1, 1, 0)$, and $(-1/2, 1, -2)$ under $(U(1)_{B-L}, A_4, -k)$, respectively, in addition to the SM Higgs $H \equiv [h^+, (v_H + h + iz)/\sqrt{2}]^T$, where H is totally neutral under $U(1)_{B-L} \otimes A_4 \otimes (-k)$. h^+ and z, z' are absorbed by the charged gauge boson W^+ and the two neutral gauge bosons Z, Z' to get masses, respectively, after spontaneous symmetry breaking of electroweak and $U(1)_{B-L}$ symmetry. φ plays a role in breaking the gauged $U(1)_{B-L}$ symmetry spontaneously, while η is expected to be an inert boson that contributes to the active neutrino mass matrix together with χ and neutral heavier fermions. Field contents and their assignments are summarized in Table I.

² More systematic analysis for quark and lepton has been done by ref. [32].

Under these symmetries, the valid Higgs potential is given by

$$V = \frac{Y_1^{(4)}}{2} \mu \varphi \chi^2 + \frac{a}{4} Y_1^{(6)} (H^\dagger \eta)^2 + \text{h.c.} \quad (1)$$

Due to the above terms, we have mass differences between the real part and the imaginary one for the neutral components of η and χ , respectively. Once we define these mass eigenstates to be m_{η_R} , m_{η_I} , m_{χ_R} , and m_{χ_I} , the mass differences are respectively given by

$$\delta m_\chi^2 \equiv m_{\chi_R}^2 - m_{\chi_I}^2 = Y_1^{(4)} \mu v' / \sqrt{2}, \quad \delta m_\eta^2 \equiv m_{\eta_R}^2 - m_{\eta_I}^2 = a(Y_1^{(6)}) v_H^2 / 4. \quad (2)$$

Notice here that these mass differences δm_χ^2 and δm_η^2 are respectively crucial in the light DM mass and active neutrino mass matrix, since they are proportional to these mass differences.

We show each of the allowed Lagrangian in the lepton sector that is invariant under these symmetries. One of the Yukawa Lagrangian is given by

$$\begin{aligned} & (Y_3^{(4)})^* \otimes \bar{L}_L \otimes N_R \otimes \tilde{\eta} + \text{h.c.} \\ &= \alpha_\eta \bar{L}_{L_1} \tilde{\eta} (y'_1 N_{R_1} + y'_2 N_{R_2} + y'_3 N_{R_3}) + \beta_\eta \bar{L}_{L_2} \tilde{\eta} (y'_1 N_{R_2} + y'_3 N_{R_1} + y'_2 N_{R_3}) \\ &+ \gamma_\eta \bar{L}_{L_3} \tilde{\eta} (y'_1 N_{R_3} + y'_3 N_{R_2} + y'_2 N_{R_1}) + \text{h.c..} \end{aligned} \quad (3)$$

Here, $\tilde{\eta} \equiv i\sigma_2 \eta^*$, being σ_2 second Pauli matrix, we define $Y_3^{(4)} \equiv [y'_1, y'_2, y'_3]^T$ and $\alpha_\eta, \beta_\eta, \gamma_\eta$ are real free parameters without loss of generality. Then the Yukawa coupling is given by

$$f = \begin{bmatrix} \alpha_\eta & 0 & 0 \\ 0 & \beta_\eta & 0 \\ 0 & 0 & \gamma_\eta \end{bmatrix} \begin{bmatrix} y'^*_1 & y'^*_2 & y'^*_3 \\ y'^*_3 & y'^*_1 & y'^*_2 \\ y'^*_2 & y'^*_3 & y'^*_1 \end{bmatrix} = \alpha_\eta \begin{bmatrix} 1 & 0 & 0 \\ 0 & \tilde{\beta}_\eta & 0 \\ 0 & 0 & \tilde{\gamma}_\eta \end{bmatrix} \begin{bmatrix} y'^*_1 & y'^*_2 & y'^*_3 \\ y'^*_3 & y'^*_1 & y'^*_2 \\ y'^*_2 & y'^*_3 & y'^*_1 \end{bmatrix} = \alpha_\eta \tilde{f}, \quad (4)$$

where $\tilde{\beta}_\eta \equiv \beta_\eta / \alpha_\eta$ and $\tilde{\gamma}_\eta \equiv \gamma_\eta / \alpha_\eta$. This coupling plays a role in connecting the active neutrino masses and new fields.

The Second Yukawa Lagrangian is given by

$$\begin{aligned} & Y_3^{(4)} \otimes \bar{N}_R \otimes S_L \otimes \chi + Y_3^{(4)} \otimes \bar{N}_R \otimes S_L \otimes \chi + Y_1^{(4)} \otimes \bar{N}_R \otimes S_L \otimes \chi + Y_{1'}^{(4)} \otimes \bar{N}_R \otimes S_L \otimes \chi + \text{h.c.} \\ &= \alpha_N [f'_1 (2\bar{N}_{R_1} S_{L_1} - \bar{N}_{R_2} S_{L_2} - \bar{N}_{R_3} S_{L_3}) + f'_2 (2\bar{N}_{R_3} S_{L_2} - \bar{N}_{R_2} S_{L_1} - \bar{N}_{R_1} S_{L_3}) \\ &+ f'_3 (2\bar{N}_{R_2} S_{L_3} - \bar{N}_{R_1} S_{L_2} - \bar{N}_{R_3} S_{L_1})] \chi \\ &+ \beta_N [f'_1 (\bar{N}_{R_3} S_{L_3} - \bar{N}_{R_2} S_{L_2}) + f'_2 (\bar{N}_{R_2} S_{L_1} - \bar{N}_{R_1} S_{L_3}) + f'_3 (\bar{N}_{R_1} S_{L_2} - \bar{N}_{R_3} S_{L_1})] \chi \\ &+ \gamma_N Y_1^{(4)} (\bar{N}_{R_1} S_{L_1} + \bar{N}_{R_2} S_{L_2} + \bar{N}_{R_3} S_{L_3})] \chi + \delta_N Y_{1'}^{(4)} (\bar{N}_{R_1} S_{L_3} + \bar{N}_{R_2} S_{L_2} + \bar{N}_{R_2} S_{L_1})] \chi + \text{h.c.}, \end{aligned} \quad (5)$$

where $\alpha_N, \beta_N, \gamma_N, \delta_N$ are complex free parameters. Then the corresponding Yukawa coupling is given by

$$g = \alpha_N \begin{bmatrix} 2y'_1 & -y'_3 & -y'_2 \\ -y'_2 & -y'_1 & 2y'_3 \\ -y'_3 & 2y'_2 & -y'_1 \end{bmatrix} + \beta_N \begin{bmatrix} 0 & y'_3 & -y'_2 \\ y'_2 & -y'_1 & 0 \\ -y'_3 & 0 & y'_1 \end{bmatrix} + \gamma_N \begin{bmatrix} 1 & 0 & 0 \\ 0 & 1 & 0 \\ 0 & 0 & 1 \end{bmatrix} + \delta_N \begin{bmatrix} 0 & 0 & 1 \\ 1 & 0 & 0 \\ 0 & 1 & 0 \end{bmatrix}. \quad (6)$$

The remaining terms are masses for exotic neutral fermions, and the first mass term is given by

$$\begin{aligned} & Y_3^{(2)} \otimes \bar{S}_L^C \otimes S_L \otimes \varphi + \text{h.c.} \\ &= \alpha_L [f_1(2\bar{S}_{L_1}^C S_{L_1} - \bar{S}_{L_2}^C S_{L_3} - \bar{S}_{L_3}^C S_{L_2}) + f_2(2\bar{S}_{L_2}^C S_{L_2} - \bar{S}_{L_3}^C S_{L_1} - \bar{S}_{L_1}^C S_{L_3}) \\ &+ f_3(2\bar{S}_{L_3}^C S_{L_3} - \bar{S}_{L_1}^C S_{L_2} - \bar{S}_{L_2}^C S_{L_1})] \varphi, \end{aligned} \quad (7)$$

where $Y_3^{(2)} \equiv [f_1, f_2, f_3]^T$. After the spontaneous breaking of φ , we find the mass matrix for Majorana mass matrix for S_L as follows:

$$M_{S_L} = \frac{\alpha_L v'}{\sqrt{2}} \begin{bmatrix} 2y_1 & -y_3 & -y_2 \\ -y_3 & 2y_2 & -y_1 \\ -y_2 & -y_1 & 2y_3 \end{bmatrix}. \quad (8)$$

M_{S_L} with 3×3 is diagonalized by a unitary matrix V_L as $D_{S_L} \equiv V_L^T M_{S_L} V_L$ and $S_L = V_L \psi_L$, where D_L is mass eigenvalue and ψ_L is mass eigenstate.

The Majorana mass term on S_R is directly given by

$$M_{S_R} \bar{S}_R^C \otimes S_R + \text{h.c.} = M_{S_R} \bar{S}_R^C \begin{bmatrix} 1 & 0 & 0 \\ 0 & 0 & 1 \\ 0 & 1 & 0 \end{bmatrix} S_R. \quad (9)$$

M_{S_R} with 3×3 is diagonalized by a unitary matrix V_R as $D_{S_R} \equiv V_R^T M_{S_R} V_R$ and $S_R = V_R \psi_R$, where D_R is mass eigenvalue and ψ_R is mass eigenstate. The concrete mass eigenstate and its mass eigenvalues are given by

$$V_R = \begin{bmatrix} 1 & 0 & 0 \\ 0 & 1/\sqrt{2} & -i/\sqrt{2} \\ 0 & 1/\sqrt{2} & i/\sqrt{2} \end{bmatrix}, \quad D_{S_R} = M_{S_R} \text{Diag}[1, 1, 1]. \quad (10)$$

Notice here that we do not have any other terms such as $\bar{N}_R^C N_R$, $\bar{S}_L S_R$, $\bar{S}_L N_R$, $\bar{S}_R^C N_R$ at tree level, but only the $\bar{N}_R^C N_R$ is generated at one-loop level. $\bar{N}_R^C N_R$ is found via the one-loop level through the following Yukawa term:

$$\begin{aligned} \bar{N}_{R_i} g_{ij} S_{L_j} (\chi_R + i\chi_I) / \sqrt{2} + \text{h.c.} &= \bar{N}_{R_i} g_{ij} V_{L_{jk}} \psi_{L_k} (\chi_R + i\chi_I) / \sqrt{2} + \text{h.c.} \\ &= \bar{N}_{R_i} G_{ik} \psi_{L_k} (\chi_R + i\chi_I) + \text{h.c.}, \end{aligned} \quad (11)$$

where $G_{ik} \equiv \sum_{j=1}^3 g_{ij} V_{L_{jk}} / \sqrt{2}$. Then the mass matrix of N_R is found as follows:

$$M_{N_{ab}} = \frac{1}{(4\pi)^2} \sum_{k=1}^3 G_{ak} D_{S_{L_k}} G_{kb}^T \left[\frac{m_{\chi_R}^2}{m_{\chi_R}^2 - D_{S_{L_k}}^2} \ln \left(\frac{m_{\chi_R}^2}{D_{S_{L_k}}^2} \right) - \frac{m_{\chi_I}^2}{m_{\chi_I}^2 - D_{S_{L_k}}^2} \ln \left(\frac{m_{\chi_I}^2}{D_{S_{L_k}}^2} \right) \right]. \quad (12)$$

M_N with 3×3 is diagonalized by a unitary matrix V_N as $D_N \equiv V_N^T M_N V_N$ and $N_R = V_N \psi_N$, where D_N is mass eigenvalue and ψ_N is mass eigenstate.

B. Dark matter

What is the DM candidate in the model? In Table I, the bosons η, φ, χ , and the fermion $S_{L_a}, S_{R_a}, N_{R_a}$ are neutral components. The lightest one of S_{L_a} and S_{R_a} would not be a natural DM candidate, since it has a mass at tree level. Naively, N_R , i.e., ψ_N in the mass eigenstate, is supposed to be relatively light because its mass is loop induced. However, their interactions are restricted by neutrino physics, as we will discuss later. As a consequence, its relic abundance via freeze-out mechanism is much larger than the Planck observation. The coupling is too small to produce the appropriate relic abundance by freeze-out mechanism, however, note that it is not feebly enough to accommodate the abundance via the freeze-in mechanism. Therefore other components than ψ_N should be the DM in the model. Hence, we consider the lightest component of χ to be DM. Let us suppose the parameter $Y_1^{(4)} \mu v'$ are positive for simplicity, then χ_I is the DM candidate.

1. Numerical analysis of χ

Even though χ has a mass at tree-level, we have an upper bound that DM mass should not exceed the mass of the lightest ψ_N . This is because χ directly interacts with ψ_N as can

be seen in Eq.(11), and lighter one has to remain in the current Universe. Here, we fix the lightest mass of ψ_N to be more than 50 GeV.

In Figure 1, it is shown that the relic abundance of the DM candidate χ_I produced by the freeze-out mechanism is shown. The relic abundance and spin-independent cross section are calculated using MicrOmegas code [90] by inputting the Lagrangian in the model. The parameter space is scanned by random number parameters in the range:

$$m_{\chi_I} = [0.01, 50] \text{ GeV}, \quad m_\phi = [0.01, 50] \text{ GeV}, \quad (13)$$

$$g_\varphi = [10^{-3}, 2\pi], \quad Y_1^{(4)} = [10^{-4}, 10^{-2}], \quad (14)$$

$$\mu v' = [10^{-5}, 10^4] \text{ GeV}^2, \quad \sin x = [-0.1, 0.1], \quad (15)$$

where x is mixing angle of neutral scalar φ and Higgs boson, which would be examined by the direct detection constraint. Red and gray points represent the allowed region where the relic abundance agrees with the observed relic abundance $\Omega h^2 = 0.120 \pm 0.001$ [91] in 3σ , and is smaller than the constraint, respectively. In all the parameter regions, there are points where the relic abundance matches the observation. The associated main annihilation process is $\chi_I \chi_I \rightarrow \varphi \rightarrow \varphi \varphi$. Its thermally averaged annihilation cross section in the non-relativistic limit is

$$\langle \sigma v_{\text{M}\ddot{\text{o}}l} \rangle \simeq \frac{g_\varphi^2 v'^2 Y_1^{(4)2} \mu^2}{1024\pi m_{\chi_I}^2 (4m_{\chi_I}^2 - m_\varphi^2)^2}, \quad (16)$$

where $\langle \dots \rangle$ represents the thermally averaged [92] and $v_{\text{M}\ddot{\text{o}}l}$ is the Møller velocity of DM.

Notice that even though φ is neutral and lighter than χ components, it cannot be a DM candidate because it is not stable. In Figure 1, the mass of φ is smaller than that of χ_I .

In Figure 2, constraint for spin-independent cross section of DM-proton interaction for direct detection is shown with current limits. In the figure, constraints are represented for cosmic-ray accelerated DM in red straight line, Xenon1T light DM search in magenta dashed line [93], Xenon1T in magenta dotted line [94, 95], DarkSide-50 in blue dashed line [96–98], CDMSlite in green dotted line [99], CRESST-III in black dashed line [100] and in black straight line [101], respectively. As well as the Figure 1, red and gray points correspond to parameter sets with which the relic abundance agrees with the constraint and is smaller than the constraints, respectively. DM χ does not directly couple to the standard model fields; thus, the only allowed interaction is through small χ_I -Higgs mixing, $\sin x$ in Eq.(15). We can see there are enough parameter points not only in the small mass region where it is

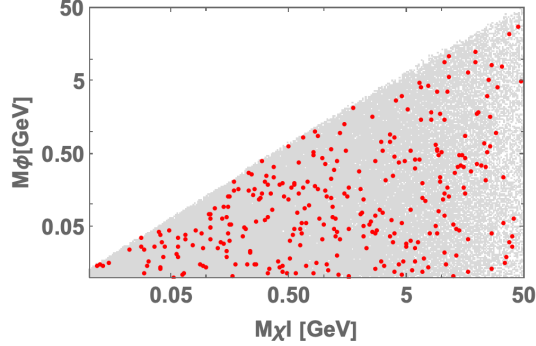


FIG. 1: Relic abundance of DM χ_I . Red and gray points represent the points where the relic abundance agrees with the observation and is smaller than that, respectively.

moderately bounded by the cosmic ray accelerated DM but also in the larger mass region than that where direct detection experiments seriously restrict it. In the points which satisfy both relic abundance and direct detection constraints, the coupling g_φ should not be too small. At the same time, the mixing angle $\sin x$ should be slight to avoid the direct detection constraints.

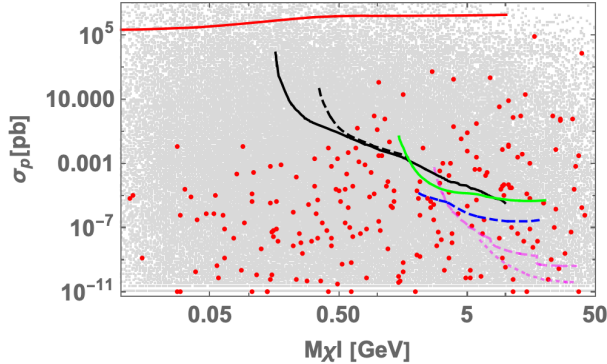


FIG. 2: The spin-independent dark matter-proton cross section associated with constraints by the direct detection. Lines represent the constraints of direct detections. See the text for details of them.

C. Neutrino sector

Similar to the N_R , we can derive the active neutrino mass matrix.

1. Neutrino mass matrix

The valid Lagrangian is now given in terms of ψ_N as follows:

$$\frac{1}{\sqrt{2}} f_{ia} \bar{\nu}_{L_i} V_{N_{ak}} \psi_{N_k} (\eta_R - \eta_I) + \text{h.c.} \equiv F_{ik} \bar{\nu}_{L_i} \psi_{N_k} (\eta_R - \eta_I) + \text{h.c.}, \quad (17)$$

where $F_{ik} \equiv \sum_{a=1}^3 f_{ia} V_{L_{ak}} / \sqrt{2} \equiv \alpha_\eta \sum_{a=1}^3 \tilde{f}_{ia} V_{L_{ak}} / \sqrt{2} \equiv \alpha_\eta \tilde{F}$. Then, the neutrino mass matrix is given at one-loop level as follows:

$$m_{\nu_{ij}} = \frac{\alpha_\eta^2}{(4\pi)^2} \sum_{k=1}^3 \tilde{F}_{ik} D_{N_k} \tilde{F}_{kj}^T \left[\frac{m_{\eta_R}^2}{m_{\eta_R}^2 - D_{N_k}^2} \ln \left(\frac{m_{\eta_R}^2}{D_{N_k}^2} \right) - \frac{m_{\eta_I}^2}{m_{\eta_I}^2 - D_{N_k}^2} \ln \left(\frac{m_{\eta_I}^2}{D_{N_k}^2} \right) \right] \equiv \alpha_\eta^2 \tilde{m}_{\nu_{ij}}. \quad (18)$$

m_ν is diagonalized by a unitary matrix U_{PMNS} [102]; $D_\nu = \alpha_\eta^2 \tilde{D}_\nu = U_{\text{PMNS}}^T m_\nu U_{\text{PMNS}} = \alpha_\eta^2 U_{\text{PMNS}}^T \tilde{m}_\nu U_{\text{PMNS}}$. Then α_η is determined by

$$(\text{NH}) : \alpha_\eta^4 = \frac{|\Delta m_{\text{atm}}^2|}{\tilde{D}_{\nu_3}^2 - \tilde{D}_{\nu_1}^2}, \quad (\text{IH}) : \alpha_\eta^4 = \frac{|\Delta m_{\text{atm}}^2|}{\tilde{D}_{\nu_2}^2 - \tilde{D}_{\nu_3}^2}, \quad (19)$$

where Δm_{atm}^2 is atmospheric neutrino mass difference squares, and NH and IH represent the normal hierarchy and the inverted hierarchy, respectively. Subsequently, the solar mass different squares can be written in terms of α_η as follows:

$$\Delta m_{\text{sol}}^2 = \alpha_\eta^4 (\tilde{D}_{\nu_2}^2 - \tilde{D}_{\nu_1}^2), \quad (20)$$

which can be compared to the observed value. In our model, one finds $U_{\text{PMNS}} = V_\nu$ since the charged-lepton is diagonal basis, and it is parametrized by three mixing angle θ_{ij} ($i, j = 1, 2, 3; i < j$), one CP violating Dirac phase δ_{CP} , and two Majorana phases $\{\alpha_{21}, \alpha_{32}\}$ as follows:

$$U_{\text{PMNS}} = \begin{pmatrix} c_{12}c_{13} & s_{12}c_{13} & s_{13}e^{-i\delta_{CP}} \\ -s_{12}c_{23} - c_{12}s_{23}s_{13}e^{i\delta_{CP}} & c_{12}c_{23} - s_{12}s_{23}s_{13}e^{i\delta_{CP}} & s_{23}c_{13} \\ s_{12}s_{23} - c_{12}c_{23}s_{13}e^{i\delta_{CP}} & -c_{12}s_{23} - s_{12}c_{23}s_{13}e^{i\delta_{CP}} & c_{23}c_{13} \end{pmatrix} \begin{pmatrix} 1 & 0 & 0 \\ 0 & e^{i\frac{\alpha_{21}}{2}} & 0 \\ 0 & 0 & e^{i\frac{\alpha_{31}}{2}} \end{pmatrix}, \quad (21)$$

where c_{ij} and s_{ij} stands for $\cos \theta_{ij}$ and $\sin \theta_{ij}$ respectively. Then, each of mixing is given in terms of the component of U_{PMNS} as follows:

$$\sin^2 \theta_{13} = |(U_{\text{PMNS}})_{13}|^2, \quad \sin^2 \theta_{23} = \frac{|(U_{\text{PMNS}})_{23}|^2}{1 - |(U_{\text{PMNS}})_{13}|^2}, \quad \sin^2 \theta_{12} = \frac{|(U_{\text{PMNS}})_{12}|^2}{1 - |(U_{\text{PMNS}})_{13}|^2}. \quad (22)$$

Also, we compute the Jarlskog invariant, δ_{CP} derived from PMNS matrix elements $U_{\alpha i}$:

$$J_{CP} = \text{Im}[U_{e1}U_{\mu 2}U_{e2}^*U_{\mu 1}^*] = s_{23}c_{23}s_{12}c_{12}s_{13}c_{13}^2 \sin \delta_{CP}, \quad (23)$$

and the Majorana phases are also estimated in terms of other invariants I_1 and I_2 :

$$I_1 = \text{Im}[U_{e1}^*U_{e2}] = c_{12}s_{12}c_{13}^2 \sin \left(\frac{\alpha_{21}}{2} \right), \quad I_2 = \text{Im}[U_{e1}^*U_{e3}] = c_{12}s_{13}c_{13} \sin \left(\frac{\alpha_{31}}{2} - \delta_{CP} \right). \quad (24)$$

In addition, the effective mass for the neutrinoless double beta decay is given by

$$\langle m_{ee} \rangle = |\alpha_\eta|^2 |\tilde{D}_{\nu_1} \cos^2 \theta_{12} \cos^2 \theta_{13} + \tilde{D}_{\nu_2} \sin^2 \theta_{12} \cos^2 \theta_{13} e^{i\alpha_{21}} + \tilde{D}_{\nu_3} \sin^2 \theta_{13} e^{i(\alpha_{31}-2\delta_{CP})}|, \quad (25)$$

where its observed value could be measured by KamLAND-Zen in future [103]. We will adopt the neutrino experimental data at 3σ interval in NuFit5.0 [104] as follows:

$$\text{NH} : \Delta m_{\text{atm}}^2 = [2.431, 2.598] \times 10^{-3} \text{ eV}^2, \quad \Delta m_{\text{sol}}^2 = [6.82, 8.04] \times 10^{-5} \text{ eV}^2, \quad (26)$$

$$\sin^2 \theta_{13} = [0.02034, 0.02430], \quad \sin^2 \theta_{23} = [0.407, 0.618], \quad \sin^2 \theta_{12} = [0.269, 0.343],$$

$$\text{IH} : \Delta m_{\text{atm}}^2 = [2.412, 2.583] \times 10^{-3} \text{ eV}^2, \quad \Delta m_{\text{sol}}^2 = [6.82, 8.04] \times 10^{-5} \text{ eV}^2, \quad (27)$$

$$\sin^2 \theta_{13} = [0.02053, 0.02436], \quad \sin^2 \theta_{23} = [0.411, 0.621], \quad \sin^2 \theta_{12} = [0.269, 0.343].$$

2. Numerical analysis

Here, we present our numerical analysis applying the following ranges of input parameters,

$$\begin{aligned} \{|\alpha_N|, |\beta_N|, |\gamma_N|, |\delta_N|\} &\in [0.0001, 1], \quad \{\tilde{\beta}_\eta, \tilde{\gamma}_\eta\} \in [0.1, 10], \quad \alpha_L \in [0.0001, 1], \\ M_{S_R} &\in [10^2, 10^{10}] \text{ GeV}, \quad m_\eta \in [10^5, 10^6] \text{ GeV}, \quad m_{\chi_R} \in [10^3, 10^5] \text{ GeV}, \end{aligned} \quad (28)$$

where in our work, we run whole the fundamental region of τ , and fix $v' = 10^5$ GeV.

Normal hierarchy case: In Fig. 3, scatter plots of $\text{Re}[\tau] \equiv \tau_{\text{Re}}$ and $\text{Im}[\tau] \equiv \tau_{\text{Im}}$ are shown, where the left up figure is the one for $m_\chi = 0.01$ GeV, the right up one $m_\chi = 0.1$ GeV, the left down one $m_\chi = 5$ GeV, and the right down one $m_\chi = 50$ GeV. Each of the allowed regions is at nearby $|\tau_{\text{Re}}| = [0.07 - 0.5]$ and $\tau_{\text{Im}} = [1.7 - 2.1]$ for $m_\chi = 0.01$ GeV, $|\tau_{\text{Re}}| = [0.05 - 0.35]$ and $\tau_{\text{Im}} = [1.5 - 2.1]$ for $m_\chi = 0.1$ GeV, $|\tau_{\text{Re}}| = [0.02 - 0.1]$ and $\tau_{\text{Im}} = [1.5 - 2.1]$ for $m_\chi = 5$ GeV, and $|\tau_{\text{Re}}| = [0.02 - 0.5]$ and $\tau_{\text{Im}} = [1.6 - 2.1]$ for $m_\chi = 50$ GeV.

In Fig. 4, scatter plots of sum of neutrino masses $\equiv \sum m$ eV and δ_{CP}^ℓ are shown, where the legends are the same as Fig. 3. Allowed regions are as follows: $\sum m = [0.075 - 0.105]$

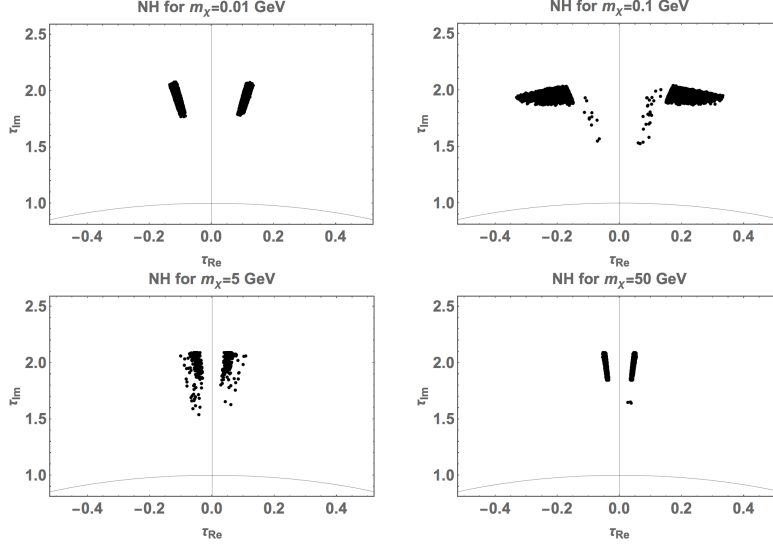


FIG. 3: Scatter plots of $\text{Re}[\tau] \equiv \tau_{\text{Re}}$ and $\text{Im}[\tau] \equiv \tau_{\text{Im}}$, where the left up figure is the one for $m_\chi = 0.01$ GeV, the right up one $m_\chi = 0.1$ GeV, the left down one $m_\chi = 5$ GeV, and the right down one $m_\chi = 50$ GeV.

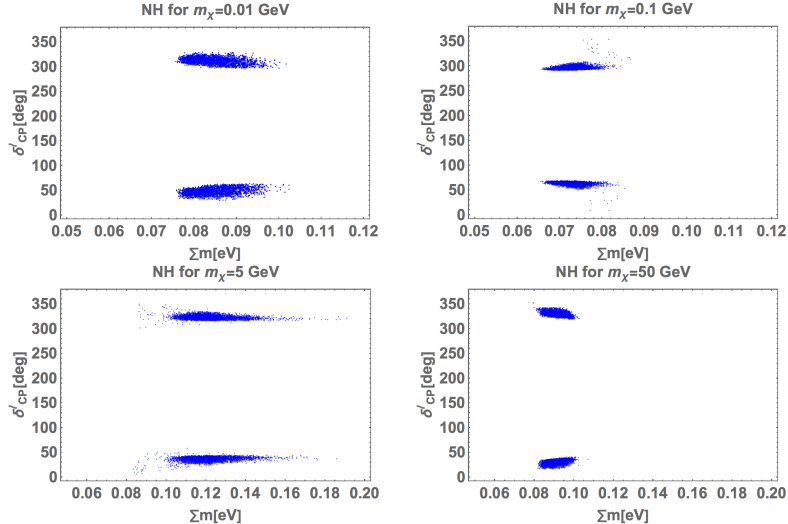


FIG. 4: Scatter plots of sum of neutrino masses $\equiv \sum m$ eV and δ_{CP}^ℓ , where the legends are the same as Fig. 3.

eV and $\delta_{\text{CP}}^\ell = [30 - 60, 300 - 330]$ for $m_\chi = 0.01$ GeV, $\sum m = [0.065 - 0.085]$ eV and $\delta_{\text{CP}}^\ell = [0 - 70, 300 - 360]$ for $m_\chi = 0.1$ GeV, $\sum m = [0.08 - 0.19]$ eV and $\delta_{\text{CP}}^\ell = [0 - 60, 300 - 360]$ for $m_\chi = 5$ GeV, and $\sum m = [0.08 - 0.11]$ eV and $\delta_{\text{CP}}^\ell = [30 - 50, 320 - 350]$ for $m_\chi = 50$ GeV.

In Fig. 5, scatter plots of $\sin^2 \theta_{23}$ and $\sum m$ are shown, where the legends are the same as Fig. 3. Allowed regions are as follows: $\sin^2 \theta_{23} = [0.407 - 0.618]$ for $m_\chi = 0.01$ GeV,

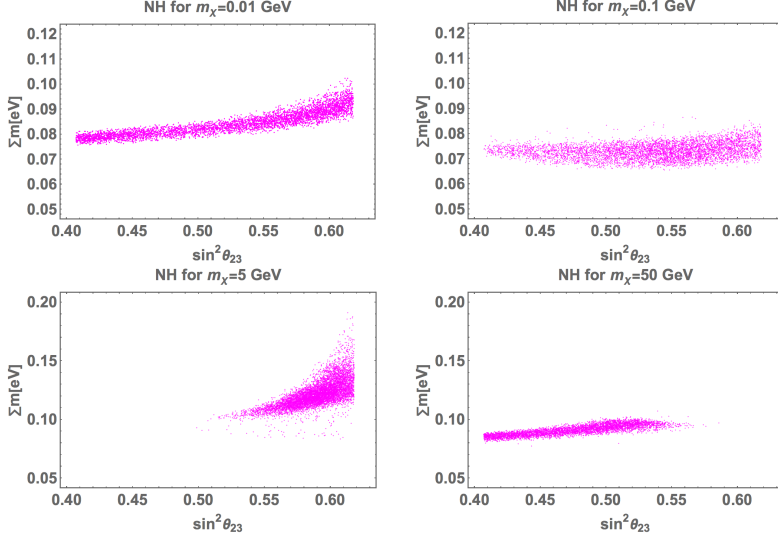


FIG. 5: Scatter plots of $\sin^2 \theta_{23}$ and $\sum m$, where the legends are the same as Fig. 3.

$\sin^2 \theta_{23} = [0.407 - 0.618]$ for $m_\chi = 0.1$ GeV, $\sin^2 \theta_{23} = [0.5 - 0.618]$ for $m_\chi = 5$ GeV, and $\sin^2 \theta_{23} = [0.407 - 0.58]$ for $m_\chi = 50$ GeV.

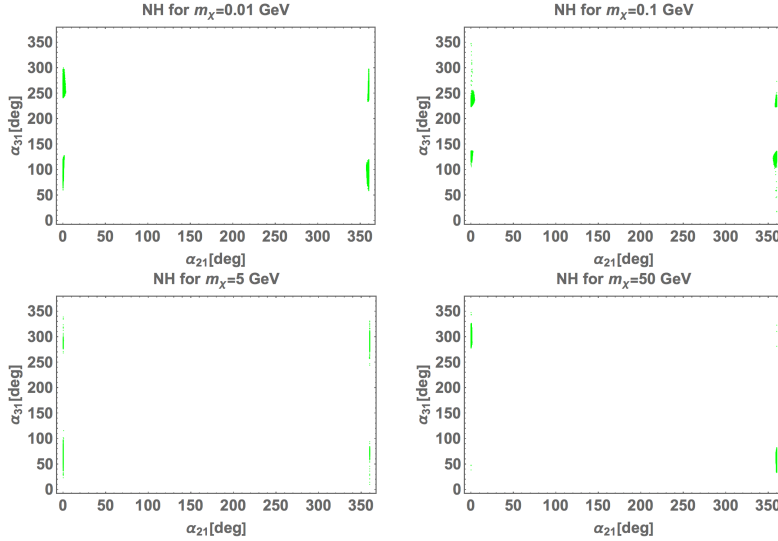


FIG. 6: Scatter plots of α_{21} [deg] and α_{31} [deg], where the legends are the same as Fig. 3.

In Fig. 6, scatter plots of α_{21} [deg] and α_{31} [deg] are shown, where the legends are the same as Fig. 3. Allowed regions are as follows: $\alpha_{21} \sim 0$ [deg] and $\alpha_{31} = [50 - 120, 240 - 300]$ [deg] for $m_\chi = 0.01$ GeV, $\alpha_{21} \sim 0$ [deg] and $\alpha_{31} = [110 - 130, 220 - 360]$ [deg] for $m_\chi = 0.1$ GeV, $\alpha_{21} \sim 0$ [deg] and $\alpha_{31} = [30 - 100, 250, 340]$ [deg] for $m_\chi = 5$ GeV, and $\alpha_{21} \sim 0$ [deg] and $\alpha_{31} = [30 - 80, 280, 350]$ [deg] for $m_\chi = 50$ GeV.

In Fig. 7, scatter plots of $\sin^2 \theta_{23}$ and $\langle m_{ee} \rangle$ are shown, where the legends are the same

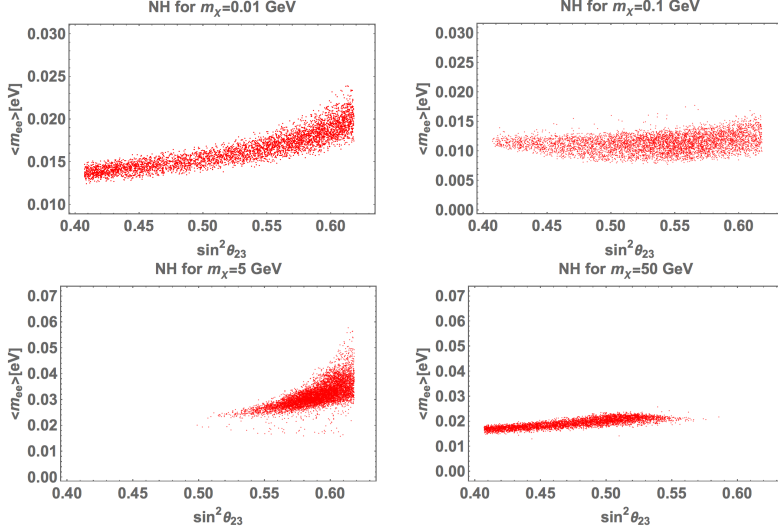


FIG. 7: Scatter plots of $\sin^2 \theta_{23}$ and $\langle m_{ee} \rangle$, where the legends are the same as Fig. 3.

as Fig. 3. Allowed regions are as follows: $\langle m_{ee} \rangle = [0.013 - 0.024]$ eV for $m_\chi = 0.01$ GeV, $\langle m_{ee} \rangle = [0.008 - 0.015]$ eV for $m_\chi = 0.1$ GeV, $\langle m_{ee} \rangle = [0.015 - 0.058]$ eV for $m_\chi = 5$ GeV, and $\langle m_{ee} \rangle = [0.016 - 0.021]$ eV for $m_\chi = 50$ GeV.

Here, we summarize some features in the case of NH. In case of $m_\chi = 5$ GeV, half of allowed region might be ruled out by the cosmological constraint $\sum m \leq 0.12$ eV and larger value of $\sin^2 \theta_{23}$ is favored. While large value of $\sin^2 \theta_{23}$ is disfavored in case of $m_\chi = 50$ GeV. For all the cases, α_{21} is almost zero, and δ_{CP} is localized at nearby 50 deg and 300 deg.

Inverted hierarchy case

In Fig. 8, scatter plots of $\text{Re}[\tau] \equiv \tau_{\text{Re}}$ and $\text{Im}[\tau] \equiv \tau_{\text{Im}}$ are shown, where the legends are the same as Fig. 3. Each of allowed regions is at nearby $|\tau_{\text{Re}}| = [0.19 - 0.21]$ and $\tau_{\text{Im}} = [1.9, 2.1]$ for $m_\chi = 0.01$ GeV, $|\tau_{\text{Re}}| = [0.19 - 0.21]$ and $\tau_{\text{Im}} = [1.9, 2.1]$ for $m_\chi = 0.1$ GeV, $|\tau_{\text{Re}}| \sim 0.2$ and $\tau_{\text{Im}} = \text{sim}$ for $m_\chi = 5$ GeV, and $|\tau_{\text{Re}}| = [0.15 - 0.23]$ and $\tau_{\text{Im}} = [1.85 - 2.1]$ for $m_\chi = 50$ GeV.

In Fig. 9, scatter plots of sum of neutrino masses $\equiv \sum m$ eV and δ_{CP}^ℓ are shown, where the legends are the same as Fig. 3. Allowed regions are as follows: $\sum m = [0.14 - 0.21]$ eV and $\delta_{CP}^\ell \sim [70, 110, 250, 290]$ for $m_\chi = 0.01$ GeV, $\sum m = [0.135 - 0.20]$ eV and $\delta_{CP}^\ell \sim [70, 120, 250, 300]$ for $m_\chi = 0.1$ GeV, $\sum m = [0.125 - 0.135]$ eV and $\delta_{CP}^\ell = [110, 250]$ for $m_\chi = 5$ GeV, and $\sum m = [0.118 - 0.175]$ eV and $\delta_{CP}^\ell = [50 - 70, 100 - 130, 230 - 260, 290 - 310]$ for $m_\chi = 50$ GeV.

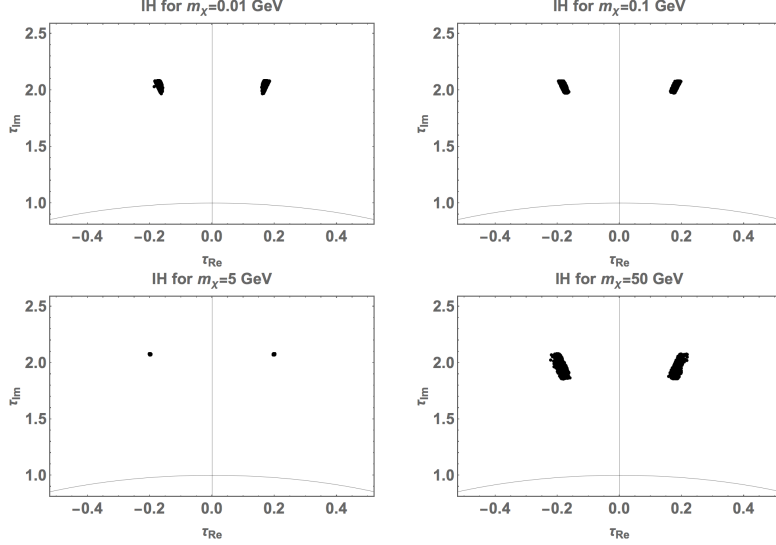


FIG. 8: Scatter plots of $\text{Re}[\tau] \equiv \tau_{\text{Re}}$ and $\text{Im}[\tau] \equiv \tau_{\text{Im}}$, where the legends are the same as Fig. 3.

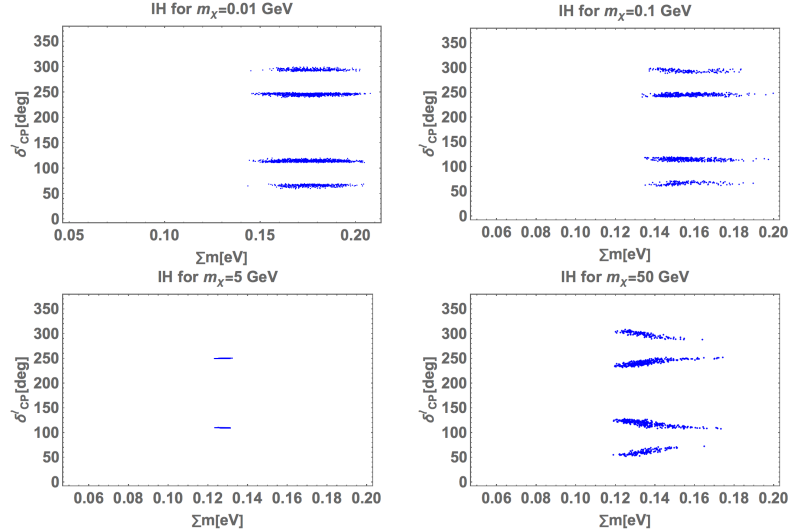


FIG. 9: Scatter plots of sum of neutrino masses $\equiv \sum m$ eV and δ^ℓ_{CP} , where the legends are the same as Fig. 3.

In Fig. 10, scatter plots of $\sin^2 \theta_{23}$ and $\sum m$ are shown, where the legends are the same as Fig. 3. Allowed regions are as follows: $\sin^2 \theta_{23} = [0.46 - 0.60]$ for $m_\chi = 0.01$ GeV, $\sin^2 \theta_{23} = [0.51 - 0.618]$ for $m_\chi = 0.1$ GeV, $\sin^2 \theta_{23} = [0.615 - 0.618]$ for $m_\chi = 5$ GeV, and $\sin^2 \theta_{23} = [0.48 - 0.618]$ for $m_\chi = 50$ GeV.

In Fig. 11, scatter plots of α_{21} [deg] and α_{31} [deg] are shown, where the legends are the same as Fig. 3. Allowed regions are as follows: $\alpha_{21} \sim 0$ [deg] and $\alpha_{31} = [120 - 140, 220 - 240]$ [deg] for $m_\chi = 0.01$ GeV, $\alpha_{21} \sim 0$ [deg] and $\alpha_{31} = [120 - 140, 220 - 240]$ [deg] for $m_\chi = 0.1$ GeV, $\alpha_{21} \sim 0$ [deg] and $\alpha_{31} = [140, 220]$ [deg] for $m_\chi = 5$ GeV, and $\alpha_{21} \sim 0$ [deg] and

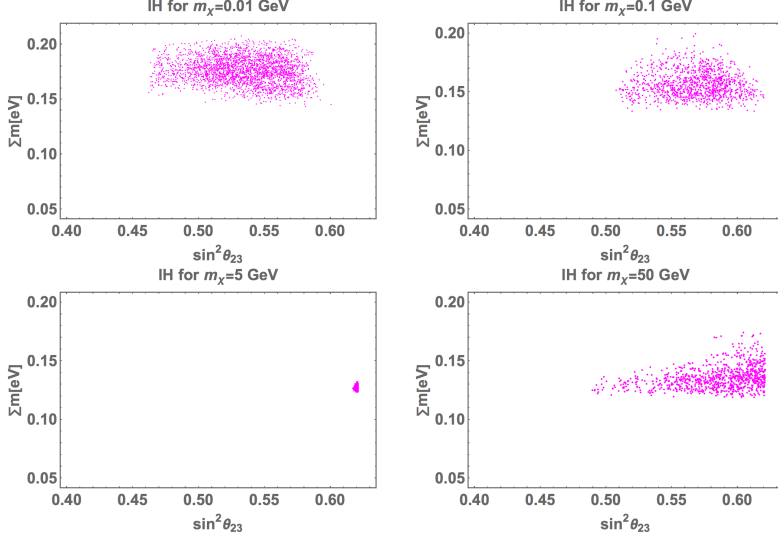


FIG. 10: Scatter plots of $\sin^2 \theta_{23}$ and $\sum m$, where the legends are the same as Fig. 3.

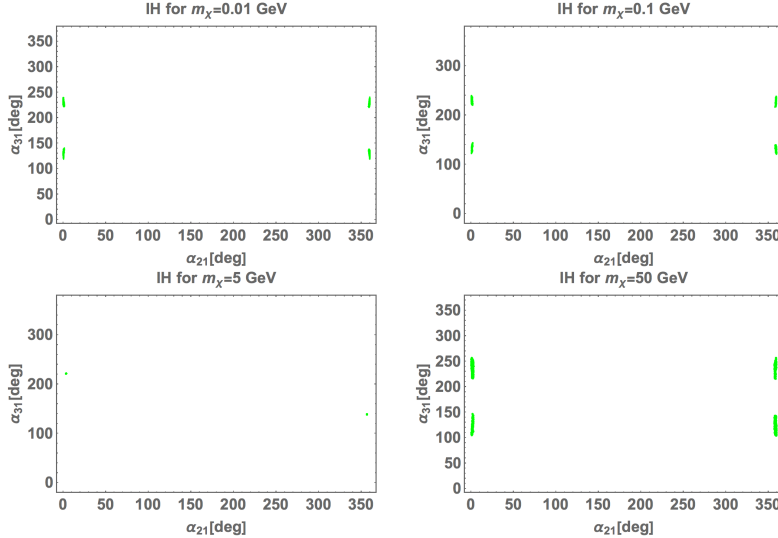


FIG. 11: Scatter plots of α_{21} [deg] and α_{31} [deg], where the legends are the same as Fig. 3.

$$\alpha_{31} = [100 - 140, 210 - 260] \text{ [deg]} \text{ for } m_\chi = 50 \text{ GeV.}$$

In Fig. 12, scatter plots of $\sin^2 \theta_{23}$ and $\langle m_{ee} \rangle$ are shown, where the legends are the same as Fig. 3. Allowed regions are as follows: $\langle m_{ee} \rangle = [0.055 - 0.07] \text{ eV}$ for $m_\chi = 0.01 \text{ GeV}$, $\langle m_{ee} \rangle = [0.055 - 0.07] \text{ eV}$ for $m_\chi = 0.1 \text{ GeV}$, $\langle m_{ee} \rangle \sim 0.053 \text{ eV}$ for $m_\chi = 5 \text{ GeV}$, and $\langle m_{ee} \rangle = [0.05 - 0.065] \text{ eV}$ for $m_\chi = 50 \text{ GeV}$.

Here, we summarize some features in the case of IH. For all the cases, τ is localized at nearby $\tau = \pm 0.2 + 2i$. In the cases of $m_\chi = 5, 50 \text{ GeV}$, there is a small allowed region to satisfy the cosmological constraint $\sum m \leq 0.12 \text{ eV}$, while there is no allowed region for the other cases. Larger value of $\sin^2 \theta_{23}$ is favored except $m_\chi = 0.01 \text{ GeV}$. For all the cases, α_{21}

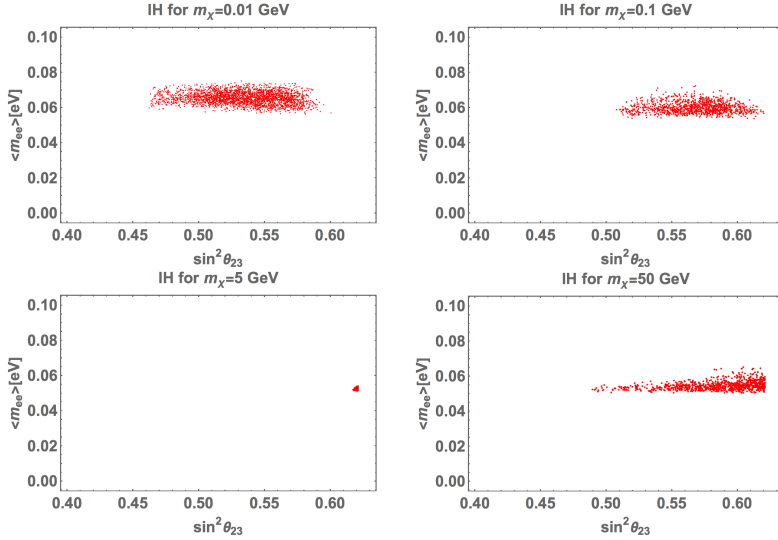


FIG. 12: Scatter plots of $\sin^2 \theta_{23}$ and $\langle m_{ee} \rangle$, where the legends are the same as Fig. 3.

is almost zero that is the same as the case of NH.

III. SUMMARY AND CONCLUSIONS

We have proposed a radiative seesaw model with a light DM candidate under the modular A_4 and gauged $U(1)_{B-L}$ symmetries, in which the neutrino masses are generated via one-loop level, and we have a relatively light bosonic DM candidate $\sim 0.01 - 50$ GeV. DM is stabilized by nonzero modular weight and a remnant Z_2 symmetry of $U(1)_{B-L}$ symmetry. The naturalness of the tiny mass of DM has indirectly been realized by the radiatively induced mass of neutral fermions that interact with our DM candidate. Thus, DM mass must not exceed the mass of the neutral fermion masses, whose scale is assumed to be 50 GeV. After checking there is a parameter space allowed by both the observations of relic density of DM and the direct detection constraints, taking four benchmark points of DM mass, we have also demonstrated the numerical analysis for the neutrino oscillation data in cases of NH and IH. We have found several features for both cases as follows.

NH case: In case of $m_\chi = 5$ GeV, half of allowed region might be ruled out by the cosmological constraint $\sum m \leq 0.12$ eV and larger value of $\sin^2 \theta_{23}$ is favored. While large value of $\sin^2 \theta_{23}$ is disfavored in case of $m_\chi = 50$ GeV. For all the cases, α_{21} is almost zero, and δ_{CP} is localized at nearby 50 deg and 300 deg.

IH case: For all the cases, τ is localized at nearby $\tau = \pm 0.2 + 2i$. In the cases of $m_\chi = 5, 50$

GeV, there is a small allowed region to satisfy the cosmological constraint $\sum m \leq 0.12$ eV, while there is no allowed region for the other cases. Larger value of $\sin^2 \theta_{23}$ is favored except $m_\chi = 0.01$ GeV. For all the cases, α_{21} is almost zero that is the same as the case of NH.

Acknowledgments

KIN was supported by JSPS Grant-in-Aid for Scientific Research (A) 18H03699, (C) 21K03562, (C) 21K03583, Okayama Foundation for Science and Technology, and Wesco Scientific Promotion Foundation. This research was supported by an appointment to the JRG Program at the APCTP through the Science and Technology Promotion Fund and Lottery Fund of the Korean Government. This was also supported by the Korean Local Governments - Gyeongsangbuk-do Province and Pohang City (H.O.). H.O. is sincerely grateful for the KIAS member.

Appendix

Here, we show several properties of modular A_4 symmetry. In general, the modular group $\bar{\Gamma}$ is a group of linear fractional transformation γ , acting on the modulus τ which belongs to the upper-half complex plane and transforms as

$$\tau \longrightarrow \gamma\tau = \frac{a\tau + b}{c\tau + d}, \quad \text{where } a, b, c, d \in \mathbb{Z} \quad \text{and} \quad ad - bc = 1, \quad \text{Im}[\tau] > 0. \quad (29)$$

This is isomorphic to $PSL(2, \mathbb{Z}) = SL(2, \mathbb{Z})/\{I, -I\}$ transformation. Then modular transformation is generated by two transformations S and T defined by:

$$S : \tau \longrightarrow -\frac{1}{\tau}, \quad T : \tau \longrightarrow \tau + 1, \quad (30)$$

and they satisfy the following algebraic relations,

$$S^2 = \mathbb{I}, \quad (ST)^3 = \mathbb{I}. \quad (31)$$

More concretely, we can fix the basis of S and T as follows:

$$S = \frac{1}{3} \begin{pmatrix} -1 & 2 & 2 \\ -2 & -1 & 2 \\ 2 & 2 & -1 \end{pmatrix}, \quad T = \begin{pmatrix} 1 & 0 & 0 \\ 0 & \omega & 0 \\ 0 & 0 & \omega^2 \end{pmatrix}, \quad (32)$$

where $\omega \equiv e^{2\pi i/3}$.

Here we introduce the series of groups $\Gamma(N)$ ($N = 1, 2, 3, \dots$) which are defined by

$$\Gamma(N) = \left\{ \begin{pmatrix} a & b \\ c & d \end{pmatrix} \in SL(2, \mathbb{Z}) , \quad \begin{pmatrix} a & b \\ c & d \end{pmatrix} = \begin{pmatrix} 1 & 0 \\ 0 & 1 \end{pmatrix} \pmod{N} \right\}, \quad (33)$$

and we define $\bar{\Gamma}(2) \equiv \Gamma(2)/\{I, -I\}$ for $N = 2$. Since the element $-I$ does not belong to $\Gamma(N)$ for $N > 2$ case, we have $\bar{\Gamma}(N) = \Gamma(N)$, that are infinite normal subgroup of $\bar{\Gamma}$ known as principal congruence subgroups. We thus obtain finite modular groups as the quotient groups defined by $\Gamma_N \equiv \bar{\Gamma}/\bar{\Gamma}(N)$. For these finite groups Γ_N , $T^N = \mathbb{I}$ is imposed, and the groups Γ_N with $N = 2, 3, 4$ and 5 are isomorphic to S_3 , A_4 , S_4 and A_5 , respectively [3].

Modular forms of level N are holomorphic functions $f(\tau)$ which are transformed under the action of $\Gamma(N)$ given by

$$f(\gamma\tau) = (c\tau + d)^k f(\tau) , \quad \gamma \in \Gamma(N) , \quad (34)$$

where k is the so-called as the modular weight.

Under the modular transformation in Eq.(29) in case of A_4 ($N = 3$) modular group, a field $\phi^{(I)}$ is also transformed as

$$\phi^{(I)} \rightarrow (c\tau + d)^{-k_I} \rho^{(I)}(\gamma) \phi^{(I)}, \quad (35)$$

where $-k_I$ is the modular weight and $\rho^{(I)}(\gamma)$ denotes a unitary representation matrix of $\gamma \in \Gamma(2)$ (A_4 representation). Thus Lagrangian, such as Yukawa terms, can be invariant if the sum of modular weight from fields and modular form in the corresponding term is zero (also invariant under A_4 and gauge symmetry).

The kinetic terms and quadratic terms of scalar fields can be written by

$$\sum_I \frac{|\partial_\mu \phi^{(I)}|^2}{(-i\tau + i\bar{\tau})^{k_I}} , \quad \sum_I \frac{|\phi^{(I)}|^2}{(-i\tau + i\bar{\tau})^{k_I}} , \quad (36)$$

which is invariant under the modular transformation and overall factor is eventually absorbed by a field redefinition consistently. Therefore the Lagrangian associated with these terms should be invariant under the modular symmetry.

The basis of modular forms with weight 2, $Y_3^{(2)} = (y_1, y_2, y_3)$, transforming as a triplet of

A_4 is written in terms of Dedekind eta-function $\eta(\tau)$ and its derivative [2]:

$$\begin{aligned} y_1(\tau) &= \frac{i}{2\pi} \left(\frac{\eta'(\tau/3)}{\eta(\tau/3)} + \frac{\eta'((\tau+1)/3)}{\eta((\tau+1)/3)} + \frac{\eta'((\tau+2)/3)}{\eta((\tau+2)/3)} - \frac{27\eta'(3\tau)}{\eta(3\tau)} \right) \\ &\simeq 1 + 12q + 36q^2 + 12q^3 + \dots , \end{aligned} \quad (37)$$

$$\begin{aligned} y_2(\tau) &= \frac{-i}{\pi} \left(\frac{\eta'(\tau/3)}{\eta(\tau/3)} + \omega^2 \frac{\eta'((\tau+1)/3)}{\eta((\tau+1)/3)} + \omega \frac{\eta'((\tau+2)/3)}{\eta((\tau+2)/3)} \right), \\ &\simeq -6q^{1/3}(1 + 7q + 8q^2 + \dots), \end{aligned} \quad (38)$$

$$\begin{aligned} y_3(\tau) &= \frac{-i}{\pi} \left(\frac{\eta'(\tau/3)}{\eta(\tau/3)} + \omega \frac{\eta'((\tau+1)/3)}{\eta((\tau+1)/3)} + \omega^2 \frac{\eta'((\tau+2)/3)}{\eta((\tau+2)/3)} \right) \\ &\simeq -18q^{2/3}(1 + 2q + 5q^2 + \dots), \end{aligned} \quad (39)$$

where $q = e^{2\pi i\tau}$, and expansion form in terms of q would sometimes be useful to have numerical analysis.

Then, we can construct the higher order of couplings $Y_1^{(4)}, Y_1^{(6)}, Y_3^{(6)}, Y_{3'}^{(6)}$ following the multiplication rules as follows:

$$Y_1^{(4)} = y_1^2 + 2y_2y_3, \quad Y_1^{(6)} = y_1^3 + y_2^3 + y_3^3 - 3y_1y_2y_3, \quad (40)$$

$$Y_3^{(6)} \equiv (y'_1, y'_2, y'_3) = (y_1^3 + 2y_1y_2y_3, y_1^2y_2 + 2y_2^2y_3, y_1^2y_3 + 2y_3^2y_2), \quad (41)$$

$$Y_{3'}^{(6)} \equiv (y''_1, y''_2, y''_3) = (y_3^3 + 2y_1y_2y_3, y_3^2y_1 + 2y_1^2y_2, y_3^2y_2 + 2y_2^2y_1), \quad (42)$$

where the above relations are constructed by the multiplication rules under A_4 as shown below:

$$\begin{aligned} \begin{pmatrix} a_1 \\ a_2 \\ a_3 \end{pmatrix}_{\mathbf{3}} \otimes \begin{pmatrix} b_1 \\ b_2 \\ b_3 \end{pmatrix}_{\mathbf{3}'} &= (a_1b_1 + a_2b_3 + a_3b_2)_{\mathbf{1}} \oplus (a_3b_3 + a_1b_2 + a_2b_1)_{\mathbf{1}'}, \\ &\oplus (a_2b_2 + a_1b_3 + a_3b_1)_{\mathbf{1}''} \\ &\oplus \frac{1}{3} \begin{pmatrix} 2a_1b_1 - a_2b_3 - a_3b_2 \\ 2a_3b_3 - a_1b_2 - a_2b_1 \\ 2a_2b_2 - a_1b_3 - a_3b_1 \end{pmatrix}_{\mathbf{3}} \oplus \frac{1}{2} \begin{pmatrix} a_2b_3 - a_3b_2 \\ a_1b_2 - a_2b_1 \\ a_3b_1 - a_1b_3 \end{pmatrix}_{\mathbf{3}'}, \end{aligned}$$

$$\mathbf{1} \otimes \mathbf{1} = \mathbf{1}, \quad \mathbf{1}' \otimes \mathbf{1}' = \mathbf{1}'', \quad \mathbf{1}'' \otimes \mathbf{1}'' = \mathbf{1}', \quad \mathbf{1}' \otimes \mathbf{1}'' = \mathbf{1}. \quad (43)$$

-
- [1] E. Ma, Phys. Rev. D **73**, 077301 (2006) doi:10.1103/PhysRevD.73.077301 [arXiv:hep-ph/0601225 [hep-ph]].
- [2] F. Feruglio, doi:10.1142/9789813238053_0012 [arXiv:1706.08749 [hep-ph]].
- [3] R. de Adelhart Toorop, F. Feruglio and C. Hagedorn, Nucl. Phys. B **858**, 437-467 (2012) doi:10.1016/j.nuclphysb.2012.01.017 [arXiv:1112.1340 [hep-ph]].
- [4] J. C. Criado and F. Feruglio, SciPost Phys. **5**, no.5, 042 (2018) doi:10.21468/SciPostPhys.5.5.042 [arXiv:1807.01125 [hep-ph]].
- [5] T. Kobayashi, N. Omoto, Y. Shimizu, K. Takagi, M. Tanimoto and T. H. Tatsuishi, JHEP **11**, 196 (2018) doi:10.1007/JHEP11(2018)196 [arXiv:1808.03012 [hep-ph]].
- [6] H. Okada and M. Tanimoto, Phys. Lett. B **791**, 54-61 (2019) doi:10.1016/j.physletb.2019.02.028 [arXiv:1812.09677 [hep-ph]].
- [7] T. Nomura and H. Okada, Phys. Lett. B **797**, 134799 (2019) doi:10.1016/j.physletb.2019.134799 [arXiv:1904.03937 [hep-ph]].
- [8] H. Okada and M. Tanimoto, Eur. Phys. J. C **81**, no.1, 52 (2021) doi:10.1140/epjc/s10052-021-08845-y [arXiv:1905.13421 [hep-ph]].
- [9] F. J. de Anda, S. F. King and E. Perdomo, Phys. Rev. D **101**, no.1, 015028 (2020) doi:10.1103/PhysRevD.101.015028 [arXiv:1812.05620 [hep-ph]].
- [10] P. P. Novichkov, S. T. Petcov and M. Tanimoto, Phys. Lett. B **793**, 247-258 (2019) doi:10.1016/j.physletb.2019.04.043 [arXiv:1812.11289 [hep-ph]].
- [11] T. Nomura and H. Okada, Nucl. Phys. B **966**, 115372 (2021) doi:10.1016/j.nuclphysb.2021.115372 [arXiv:1906.03927 [hep-ph]].
- [12] H. Okada and Y. Orikasa, [arXiv:1907.13520 [hep-ph]].
- [13] G. J. Ding, S. F. King and X. G. Liu, JHEP **09**, 074 (2019) doi:10.1007/JHEP09(2019)074 [arXiv:1907.11714 [hep-ph]].
- [14] T. Nomura, H. Okada and O. Popov, Phys. Lett. B **803**, 135294 (2020) doi:10.1016/j.physletb.2020.135294 [arXiv:1908.07457 [hep-ph]].
- [15] T. Kobayashi, Y. Shimizu, K. Takagi, M. Tanimoto and T. H. Tatsuishi, Phys. Rev. D **100**, no.11, 115045 (2019) [erratum: Phys. Rev. D **101**, no.3, 039904 (2020)] doi:10.1103/PhysRevD.100.115045 [arXiv:1909.05139 [hep-ph]].

- [16] T. Asaka, Y. Heo, T. H. Tatsuishi and T. Yoshida, JHEP **01**, 144 (2020) doi:10.1007/JHEP01(2020)144 [arXiv:1909.06520 [hep-ph]].
- [17] D. Zhang, Nucl. Phys. B **952**, 114935 (2020) doi:10.1016/j.nuclphysb.2020.114935 [arXiv:1910.07869 [hep-ph]].
- [18] G. J. Ding, S. F. King, X. G. Liu and J. N. Lu, JHEP **12**, 030 (2019) doi:10.1007/JHEP12(2019)030 [arXiv:1910.03460 [hep-ph]].
- [19] T. Kobayashi, T. Nomura and T. Shimomura, Phys. Rev. D **102**, no.3, 035019 (2020) doi:10.1103/PhysRevD.102.035019 [arXiv:1912.00637 [hep-ph]].
- [20] T. Nomura, H. Okada and S. Patra, Nucl. Phys. B **967**, 115395 (2021) doi:10.1016/j.nuclphysb.2021.115395 [arXiv:1912.00379 [hep-ph]].
- [21] X. Wang, Nucl. Phys. B **957**, 115105 (2020) doi:10.1016/j.nuclphysb.2020.115105 [arXiv:1912.13284 [hep-ph]].
- [22] H. Okada and Y. Shojo, Nucl. Phys. B **961**, 115216 (2020) doi:10.1016/j.nuclphysb.2020.115216 [arXiv:2003.13219 [hep-ph]].
- [23] H. Okada and M. Tanimoto, [arXiv:2005.00775 [hep-ph]].
- [24] M. K. Behera, S. Singirala, S. Mishra and R. Mohanta, [arXiv:2009.01806 [hep-ph]].
- [25] M. K. Behera, S. Mishra, S. Singirala and R. Mohanta, [arXiv:2007.00545 [hep-ph]].
- [26] T. Nomura and H. Okada, [arXiv:2007.04801 [hep-ph]].
- [27] T. Nomura and H. Okada, [arXiv:2007.15459 [hep-ph]].
- [28] T. Asaka, Y. Heo and T. Yoshida, Phys. Lett. B **811**, 135956 (2020) doi:10.1016/j.physletb.2020.135956 [arXiv:2009.12120 [hep-ph]].
- [29] H. Okada and M. Tanimoto, Phys. Rev. D **103**, no.1, 015005 (2021) doi:10.1103/PhysRevD.103.015005 [arXiv:2009.14242 [hep-ph]].
- [30] K. I. Nagao and H. Okada, [arXiv:2010.03348 [hep-ph]].
- [31] H. Okada and M. Tanimoto, JHEP **03**, 010 (2021) doi:10.1007/JHEP03(2021)010 [arXiv:2012.01688 [hep-ph]].
- [32] C. Y. Yao, J. N. Lu and G. J. Ding, JHEP **05** (2021), 102 doi:10.1007/JHEP05(2021)102 [arXiv:2012.13390 [hep-ph]].
- [33] P. Chen, G. J. Ding and S. F. King, JHEP **04** (2021), 239 doi:10.1007/JHEP04(2021)239 [arXiv:2101.12724 [hep-ph]].
- [34] M. Kashav and S. Verma, [arXiv:2103.07207 [hep-ph]].

- [35] H. Okada, Y. Shimizu, M. Tanimoto and T. Yoshida, [arXiv:2105.14292 [hep-ph]].
- [36] I. de Medeiros Varzielas and J. Lourenço, [arXiv:2107.04042 [hep-ph]].
- [37] T. Nomura, H. Okada and Y. Orikasa, [arXiv:2106.12375 [hep-ph]].
- [38] P. T. P. Hutařuk, D. W. Kang, J. Kim and H. Okada, [arXiv:2012.11156 [hep-ph]].
- [39] T. Kobayashi, K. Tanaka and T. H. Tatsuishi, Phys. Rev. D **98**, no.1, 016004 (2018) doi:10.1103/PhysRevD.98.016004 [arXiv:1803.10391 [hep-ph]].
- [40] T. Kobayashi, Y. Shimizu, K. Takagi, M. Tanimoto, T. H. Tatsuishi and H. Uchida, Phys. Lett. B **794**, 114-121 (2019) doi:10.1016/j.physletb.2019.05.034 [arXiv:1812.11072 [hep-ph]].
- [41] T. Kobayashi, Y. Shimizu, K. Takagi, M. Tanimoto and T. H. Tatsuishi, PTEP **2020**, no.5, 053B05 (2020) doi:10.1093/ptep/ptaa055 [arXiv:1906.10341 [hep-ph]].
- [42] H. Okada and Y. Orikasa, Phys. Rev. D **100**, no.11, 115037 (2019) doi:10.1103/PhysRevD.100.115037 [arXiv:1907.04716 [hep-ph]].
- [43] S. Mishra, [arXiv:2008.02095 [hep-ph]].
- [44] X. Du and F. Wang, JHEP **02**, 221 (2021) doi:10.1007/JHEP02(2021)221 [arXiv:2012.01397 [hep-ph]].
- [45] J. T. Penedo and S. T. Petcov, Nucl. Phys. B **939**, 292-307 (2019) doi:10.1016/j.nuclphysb.2018.12.016 [arXiv:1806.11040 [hep-ph]].
- [46] P. P. Novichkov, J. T. Penedo, S. T. Petcov and A. V. Titov, JHEP **04**, 005 (2019) doi:10.1007/JHEP04(2019)005 [arXiv:1811.04933 [hep-ph]].
- [47] T. Kobayashi, Y. Shimizu, K. Takagi, M. Tanimoto and T. H. Tatsuishi, JHEP **02**, 097 (2020) doi:10.1007/JHEP02(2020)097 [arXiv:1907.09141 [hep-ph]].
- [48] S. F. King and Y. L. Zhou, Phys. Rev. D **101**, no.1, 015001 (2020) doi:10.1103/PhysRevD.101.015001 [arXiv:1908.02770 [hep-ph]].
- [49] H. Okada and Y. Orikasa, [arXiv:1908.08409 [hep-ph]].
- [50] J. C. Criado, F. Feruglio and S. J. D. King, JHEP **02**, 001 (2020) doi:10.1007/JHEP02(2020)001 [arXiv:1908.11867 [hep-ph]].
- [51] X. Wang and S. Zhou, JHEP **05**, 017 (2020) doi:10.1007/JHEP05(2020)017 [arXiv:1910.09473 [hep-ph]].
- [52] Y. Zhao and H. H. Zhang, JHEP **03** (2021), 002 doi:10.1007/JHEP03(2021)002 [arXiv:2101.02266 [hep-ph]].
- [53] S. F. King and Y. L. Zhou, JHEP **04** (2021), 291 doi:10.1007/JHEP04(2021)291

[arXiv:2103.02633 [hep-ph]].

- [54] G. J. Ding, S. F. King and C. Y. Yao, [arXiv:2103.16311 [hep-ph]].
- [55] X. Zhang and S. Zhou, [arXiv:2106.03433 [hep-ph]].
- [56] Bu-Yao Qu, Xiang-Gan Liu, Ping-Tao Chen, Gui-Jun Ding [arXiv:2106.11659 [hep-ph]].
- [57] P. P. Novichkov, J. T. Penedo, S. T. Petcov and A. V. Titov, JHEP **04**, 174 (2019) doi:10.1007/JHEP04(2019)174 [arXiv:1812.02158 [hep-ph]].
- [58] G. J. Ding, S. F. King and X. G. Liu, Phys. Rev. D **100**, no.11, 115005 (2019) doi:10.1103/PhysRevD.100.115005 [arXiv:1903.12588 [hep-ph]].
- [59] X. Wang, B. Yu and S. Zhou, Phys. Rev. D **103**, no.7, 076005 (2021) doi:10.1103/PhysRevD.103.076005 [arXiv:2010.10159 [hep-ph]].
- [60] C. Y. Yao, X. G. Liu and G. J. Ding, Phys. Rev. D **103**, no.9, 095013 (2021) doi:10.1103/PhysRevD.103.095013 [arXiv:2011.03501 [hep-ph]].
- [61] X. Wang and S. Zhou, [arXiv:2102.04358 [hep-ph]].
- [62] M. K. Behera and R. Mohanta, [arXiv:2108.01059 [hep-ph]].
- [63] A. Baur, H. P. Nilles, A. Trautner and P. K. S. Vaudrevange, Phys. Lett. B **795**, 7-14 (2019) doi:10.1016/j.physletb.2019.03.066 [arXiv:1901.03251 [hep-th]].
- [64] I. de Medeiros Varzielas, S. F. King and Y. L. Zhou, Phys. Rev. D **101**, no.5, 055033 (2020) doi:10.1103/PhysRevD.101.055033 [arXiv:1906.02208 [hep-ph]].
- [65] X. G. Liu and G. J. Ding, JHEP **08**, 134 (2019) doi:10.1007/JHEP08(2019)134 [arXiv:1907.01488 [hep-ph]].
- [66] P. Chen, G. J. Ding, J. N. Lu and J. W. F. Valle, Phys. Rev. D **102**, no.9, 095014 (2020) doi:10.1103/PhysRevD.102.095014 [arXiv:2003.02734 [hep-ph]].
- [67] C. C. Li, X. G. Liu and G. J. Ding, [arXiv:2108.02181 [hep-ph]].
- [68] P. P. Novichkov, J. T. Penedo and S. T. Petcov, Nucl. Phys. B **963**, 115301 (2021) doi:10.1016/j.nuclphysb.2020.115301 [arXiv:2006.03058 [hep-ph]].
- [69] X. G. Liu, C. Y. Yao and G. J. Ding, Phys. Rev. D **103**, no.5, 056013 (2021) doi:10.1103/PhysRevD.103.056013 [arXiv:2006.10722 [hep-ph]].
- [70] S. Kikuchi, T. Kobayashi, H. Otsuka, S. Takada and H. Uchida, JHEP **11**, 101 (2020) doi:10.1007/JHEP11(2020)101 [arXiv:2007.06188 [hep-th]].
- [71] Y. Almumin, M. C. Chen, V. Knapp-Pérez, S. Ramos-Sánchez, M. Ratz and S. Shukla, JHEP **05** (2021), 078 doi:10.1007/JHEP05(2021)078 [arXiv:2102.11286 [hep-th]].

- [72] G. J. Ding, F. Feruglio and X. G. Liu, SciPost Phys. **10** (2021), 133 doi:10.21468/SciPostPhys.10.6.133 [arXiv:2102.06716 [hep-ph]].
- [73] F. Feruglio, V. Gherardi, A. Romanino and A. Titov, JHEP **05** (2021), 242 doi:10.1007/JHEP05(2021)242 [arXiv:2101.08718 [hep-ph]].
- [74] S. Kikuchi, T. Kobayashi and H. Uchida, [arXiv:2101.00826 [hep-th]].
- [75] P. P. Novichkov, J. T. Penedo and S. T. Petcov, JHEP **04** (2021), 206 doi:10.1007/JHEP04(2021)206 [arXiv:2102.07488 [hep-ph]].
- [76] G. Altarelli and F. Feruglio, Rev. Mod. Phys. **82**, 2701-2729 (2010) doi:10.1103/RevModPhys.82.2701 [arXiv:1002.0211 [hep-ph]].
- [77] H. Ishimori, T. Kobayashi, H. Ohki, Y. Shimizu, H. Okada and M. Tanimoto, Prog. Theor. Phys. Suppl. **183**, 1-163 (2010) doi:10.1143/PTPS.183.1 [arXiv:1003.3552 [hep-th]].
- [78] H. Ishimori, T. Kobayashi, H. Ohki, H. Okada, Y. Shimizu and M. Tanimoto, Lect. Notes Phys. **858**, 1-227 (2012) doi:10.1007/978-3-642-30805-5
- [79] D. Hernandez and A. Y. Smirnov, Phys. Rev. D **86**, 053014 (2012) doi:10.1103/PhysRevD.86.053014 [arXiv:1204.0445 [hep-ph]].
- [80] S. F. King and C. Luhn, Rept. Prog. Phys. **76**, 056201 (2013) doi:10.1088/0034-4885/76/5/056201 [arXiv:1301.1340 [hep-ph]].
- [81] S. F. King, A. Merle, S. Morisi, Y. Shimizu and M. Tanimoto, New J. Phys. **16**, 045018 (2014) doi:10.1088/1367-2630/16/4/045018 [arXiv:1402.4271 [hep-ph]].
- [82] S. F. King, Prog. Part. Nucl. Phys. **94**, 217-256 (2017) doi:10.1016/j.ppnp.2017.01.003 [arXiv:1701.04413 [hep-ph]].
- [83] S. T. Petcov, Eur. Phys. J. C **78**, no.9, 709 (2018) doi:10.1140/epjc/s10052-018-6158-5 [arXiv:1711.10806 [hep-ph]].
- [84] A. Baur, H. P. Nilles, A. Trautner and P. K. S. Vaudrevange, Nucl. Phys. B **947**, 114737 (2019) doi:10.1016/j.nuclphysb.2019.114737 [arXiv:1908.00805 [hep-th]].
- [85] T. Kobayashi, Y. Shimizu, K. Takagi, M. Tanimoto, T. H. Tatsuishi and H. Uchida, Phys. Rev. D **101**, no.5, 055046 (2020) doi:10.1103/PhysRevD.101.055046 [arXiv:1910.11553 [hep-ph]].
- [86] P. P. Novichkov, J. T. Penedo, S. T. Petcov and A. V. Titov, JHEP **07**, 165 (2019) doi:10.1007/JHEP07(2019)165 [arXiv:1905.11970 [hep-ph]].
- [87] M. Tanimoto and K. Yamamoto, [arXiv:2106.10919 [hep-ph]].

- [88] M. C. Chen, S. Ramos-Sánchez and M. Ratz, Phys. Lett. B **801**, 135153 (2020) doi:10.1016/j.physletb.2019.135153 [arXiv:1909.06910 [hep-ph]].
- [89] I. de Medeiros Varzielas, M. Levy and Y. L. Zhou, JHEP **11**, 085 (2020) doi:10.1007/JHEP11(2020)085 [arXiv:2008.05329 [hep-ph]].
- [90] G. Belanger, A. Mjallal and A. Pukhov, Eur. Phys. J. C **81**, no.3, 239 (2021) doi:10.1140/epjc/s10052-021-09012-z.
- [91] N. Aghanim *et al.* [Planck], Astron. Astrophys. **641**, A6 (2020) [erratum: Astron. Astrophys. **652**, C4 (2021)] doi:10.1051/0004-6361/201833910. Nucl. Phys. B360 (1991) 145-179.
- [92] P. Gondolo and G. Gelmini, Nucl. Phys. B **360**, 145-179 (1991) doi:10.1016/0550-3213(91)90438-4
- [93] E. Aprile *et al.* [XENON], Phys. Rev. Lett. **123**, no.25, 251801 (2019) doi:10.1103/PhysRevLett.123.251801 [arXiv:1907.11485 [hep-ex]].
- [94] E. Aprile *et al.* [XENON], Phys. Rev. Lett. **121**, no.11, 111302 (2018) doi:10.1103/PhysRevLett.121.111302.
- [95] E. Aprile *et al.* [XENON], Phys. Rev. Lett. **122**, no.14, 141301 (2019) doi:10.1103/PhysRevLett.122.141301.
- [96] P. Agnes *et al.* [DarkSide], Phys. Rev. Lett. **121**, no.11, 111303 (2018) doi:10.1103/PhysRevLett.121.111303.
- [97] P. Agnes *et al.* [DarkSide], Phys. Rev. Lett. **121**, no.8, 081307 (2018) doi:10.1103/PhysRevLett.121.081307.
- [98] P. Agnes *et al.* [DarkSide], Phys. Rev. D **98**, no.10, 102006 (2018) doi:10.1103/PhysRevD.98.102006.
- [99] R. Agnese *et al.* [SuperCDMS], Phys. Rev. Lett. **116**, no.7, 071301 (2016) doi:10.1103/PhysRevLett.116.071301
- [100] F. Petricca *et al.* [CRESST], J. Phys. Conf. Ser. **1342**, no.1, 012076 (2020) doi:10.1088/1742-6596/1342/1/012076 [arXiv:1711.07692 [astro-ph.CO]].
- [101] M. Mancuso, A. H. Abdelhameed, [...]The CRESST Collaboration, Journal of Low Temperature Physics volume 199, pages 547-555 (2020)
- [102] Z. Maki, M. Nakagawa and S. Sakata, Prog. Theor. Phys. **28**, 870-880 (1962) doi:10.1143/PTP.28.870
- [103] A. Gando *et al.* [KamLAND-Zen], Phys. Rev. Lett. **117**, no.8, 082503 (2016)

doi:10.1103/PhysRevLett.117.082503 [arXiv:1605.02889 [hep-ex]].

- [104] I. Esteban, M. C. Gonzalez-Garcia, A. Hernandez-Cabezudo, M. Maltoni and T. Schwetz,
JHEP **01**, 106 (2019) doi:10.1007/JHEP01(2019)106 [arXiv:1811.05487 [hep-ph]].